Chromium 1995

David K. Geiger *

SUNY Genesco, Dept. of Chemistry, Genesco, 1 College Circle, New York 14454-1501, U.S.A.

Contents

1. Introduction

This review covers the coordination chemistry of chromium published in 1995. Although not comprehensive, this review aims to provide a broad and representative survey of the literature of the period. Volumes 122 through 124 of *Chemical Abstracts*, *CARL UnCover Online*, and the indices of major journals in the area were used to obtain the citations included herein. In general, organometallic complexes are not

* Corresponding author. E-mail: geiger@uno.cc.genesco.edu

covered. The organization used is similar to that employed in previous years with particular emphasis placed on the ligand systems.

2. Chromium(VI)

A number of arylimido complexes of chromium(VI) were reported [1]. The synthesis of the starting materials $CrCl_2(NR)_2$, where $R = 2,4,6-C_6H_2Me_3$ and $2,6-C_6H_3Me_2$ was carried out via reaction (1). The chromium atoms exhibit distorted tetrahedral geometry in both the N^tBu and

$$CrCl_2(N^tBu)_2 + 2RNCO \rightarrow CrCl_2(NR)_2 + 2^tBuNCO \qquad (1)$$
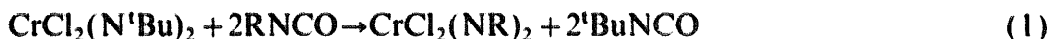
mesityl complexes. The structures contain near-linear imido ligands with Cr–N distances of 1.65 Å. Reaction of the mesitylimido complex with PMe_3 or py results in the formation of a bis adduct. NMR spectroscopic data suggest that the complexes exhibit symmetrical adduct geometries or fast interconversions in solution. Chloride substitution occurs when the mesitylimido complex is reacted with terpy and $AgBF_4$ or with sodium alkoxides or thiolates. ^1H NMR spectroscopic data are consistent with tetrahedral geometries and only one type of mesitylimido group. The structure of $Cr(2,4,6-Me_3C_6H_2O)_2(2,4,6-Me_3C_6H_2N)_2$ exhibits Cr=N and Cr–O lengths of 1.655 Å and 1.819 Å, respectively. Reaction of $CrCl_2(2,4,6-Me_3C_6H_2N)_2$ with Grignard reagents also results in substitution of the chloride ligands to give complexes of the type $Cr(2,4,6-Me_3C_6H_2N)_2R_2$ when $R = CH_2CMe_3$, CH_2CMe_2Ph, or CH_2Ph. However, use of the Grignard reagent with $R = 4-^tBuBz$ results in the formation of a Cr(IV) complex (see Section 4). Reaction of $CrCl_2(2,4,6-Me_3C_6H_2N)_2$ with MgEtBr in the presence of PMe_3 gives a dimeric Cr(V) complex (see Section 3). $Cr(2,4,6-Me_3C_6H_2N)_2(CH_2CMe_2Ph)_2$ reacts with ^tBuNC and $(2,6-xylyl)NC$ to give the iminoacyls $Cr(2,4,6-Me_3C_6H_2N)_2(CH_2CMe_2Ph)[RN=C(CH_2CMe_2Ph)]$, where $R = ^tBu$ and $2,6-Me_2C_6H_3$.

The synthesis and characterization of the bis(arylimido) complex $Cr(2,6-^iPr_2C_6H_3N)_2(NH^tBu)Cl$ was reported [2]. The structure exhibits a tetrahedral coordination geometry. Reaction of the bis(arylimido) with BCl_3 results in its conversion to $Cr(2,6-^iPr_2C_6H_3N)_2Cl_2$. The Cr=N bond lengths are 1.643 and 1.654 Å. The Cr=N–C bond angles are 157 and 159° and the Cr–N–C bond angle is 137°. The Cr–N(amide) bond distance is 1.813 Å.

The compound $[Cr(N^tBu)_2(terpy)](BF_4)_2$ was prepared from $Cr(N^tBu)_2Cl_2$ and shown to undergo imido group transfer to phosphines to give phosphinimines $^tBuN=PR_3$ [3]. The dicationic complex exhibits trigonal bipyramidal coordination geometry with the equatorial plane composed of two imide ligands and one terpyridyl nitrogen. The average Cr–N(imido) distance is 1.64 Å and the average Cr–N–C angle is 167°. The kinetics for the imido group transfer is biphasic. The results are suggestive of a two-step mechanism involving the intermediate formation of an imido Cr(IV) complex. CV studies on the dicationic complex reveal a reversible

couple at −0.74 V and an irreversible wave at −1.45 V vs Fc⁺/Fc. Reaction of $Cr(N^tBu)_2Cl_2$ and sodium 2,6-diisopropylphenoxide resulted in substitution of the chlorides with phenoxide ligands. The complex does not react with phosphines and is air-stable. CV-Analysis reveals a reversible Cr(VI)/Cr(V) couple at −1.2 V vs Fc⁺/Fc.

(1)
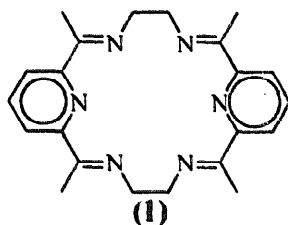
A series of chromate, dichromate, and mixed chromate–dichromate complexes were prepared from K_2CrO_4 or $K_2Cr_2O_7$ and $[ML(OAc)_2]Cl$, where M is a lanthanide(III) ion and L is the macrocycle (1) shown below [4]. Complexes with the formulas $ML(CrO_4)_{1.5} \cdot xH_2O$, $ML(Cr_2O_7)_{1.5} \cdot xH_2O$, and $ML(CrO_4)(Cr_2O_7)_{0.5} \cdot xH_2O$ were isolated. The crystal structures of three complexes were reported. The complex $[(CrO_4)LEu(\mu\text{-}CrO_4)EuL(CrO_4)] \cdot 10H_2O$ crystallizes as a centrosymmetric molecule composed of two EuL^{3+} moieties with a $\mu\text{-}CrO_4$ group that coordinates via a single oxygen atom to the Eu(III) ions. The bridging chromate is located close to a crystallographically imposed inversion centre and is present in two alternative positions. The Cr–O(bridge) bond distances are decidedly asymmetric (1.70 and 1.80 Å), whereas the Cr–O(terminal) bond distances are 1.65 and 1.64 Å. The EuL^{3+} units are somewhat folded with the concave sides of the macrocycles facing each other. The coordination spheres are completed by the didentate coordination of a chromate ligand on the convex side of each unit. The average Cr–O bridge and terminal distances are 1.67 and 1.62 Å, respectively. In the isostructural Sm(III) and Eu(III) complexes with the coordination formula $[ML(CrO_4)(H_2O)]_2Cr_2O_7 \cdot 2H_2O$, the macrocycle also adopts a folded conformation with a didentate chromate ligand present on the convex side and a water ligand on the concave side of the macrocycle. The Eu–O bond distances (2.369 and 2.386 Å) are shorter those found in the dimer (2.450 and 2.392 Å). The average chromate Cr–O bridge and terminal distances are 1.67 and 1.62 Å. The dichromate counter-ion is disordered about a centre of symmetry. The structure of the complex $[TbL(CrO_4)(H_2O)]_2Cr_2O_7 \cdot 2H_2O$ was also reported [5]. The structure is similar to the Sm(III) and Eu(III) complexes with average Tb-O bridge and terminal distances of 1.66 and 1.62 Å.

The crystal structure of wattersite, $Hg^I_4Hg^{II}Cr^{VI}O_6$, was determined [6]. A representation of the coordination polyhedra of the cations is shown in (2). Three distinct Hg sites are found in the structure. A Hg–Hg (2.526 Å) bond exists between the Hg(I) centres. One of the Hg(I) centres is four-coordinate and the other is five-coordinate. The Hg(II) ion possesses an octahedral coordination geometry composed of oxide ions. Adjacent HgO_6 octahedra share edges and are bridged to

CrO_4 tetrahedra by oxides. The overall structure is thus composed of chains of $[HgCrO_6]^{6-}$ linked to the mercury dimer by O–Hg bonds.

(2)
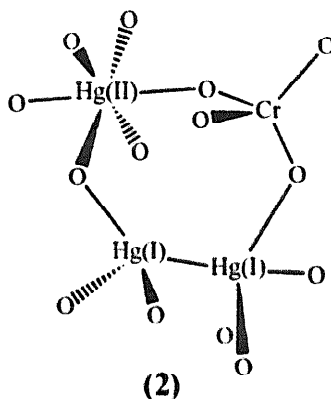
A study of the interaction of Cr(VI) and d-tartaric or dl-mandelic acid by spectroscopy was reported [7]. Spectra suggest a weak interaction between the Cr(VI) and the ligands. However, Cr(III) bands are observed in the UV–VIS spectra and the presence of benzaldehyde was detected in the mandelic acid system, suggesting that the mandelic acid is oxidized by the Cr(IV).

Reversed-phase ion-pair chromatography has been used for the simultaneous separation and determination of Cr(III), Cr(VI) and common ions [8]. The methodology takes advantage of the formation of Cr complexes with 1,2-diaminecyclohexane-N,N,N',N'-tetraacetic acid, DCTA. The detection limits was 35 ng mL^{-1} for Cr(VI), respectively. Studies of pH dependence were reported. The in vitro reduction of potassium chromate with biomimetic components was examined [9]. The biomimetic components examined were the thiol-containing molecules l-cys, l-cys ethyl ester, and glutathione; ascorbic acid; saccharides (hexoses and pentoses) and their derivatives; and nucleotides and their components. The reduction of the chromate to Cr(III) was monitored by UV–VIS spectroscopy. An intermediate Cr(V) species was observed in the spectra and by EPR spectroscopy. The trend in chromate reduction followed the order ascorbic acid > thiols ≫ saccharides and derivatives > nucleotides.

Investigations of the effect of reduction of Cr(VI) by ascorbate, asc, on DNA were reported [10]. The reduction leads to the induction of apurinic/apyrimidinic sites (AP-sites) as well as single-strand breaks. Protection of the AP-sites from putrescine-mediated DNA cleavage by prior reduction with NaBH$_4$ was used to infer the presence of aldehyde groups. The two types of lesions were induced with equal probability, suggesting a link in their generation. The authors speculate that both lesions arise from attack by a single reactive species on one site of DNA. The reduction of Cr(IV) to Cr(III) by sodium perborate was studied in acidic solution at various pHs [11]. The process was monitored by UV–VIS spectroscopy. The process is believed to go through an oxodiperoxochromium(VI) intermediate.

The effects of ascorbic acid and reduced glutathione on the induction of DNA-protein cross-links by chromate were examined [12]. Glutathione was shown to have

a concentration-dependent effect on the formation of cross-links. However, pretreatment with the monoethylester of glutathione did not increase the Cr(VI) induced cross-linking in the presence of ascorbyl palmitate. Results from chromium uptake studies indicate a binding of chromium species to DNA or protein. The uptake of chromate into HL-60 cells was raised by glutathione.

Evidence was presented that exposure of intact cells to chromate results in the formation of DNA adducts involving chromium and free amino acids or glutathione [13]. The amount of cross-linking of glutathione to DNA was chromate dose dependent. Data suggest that the ternary complexes formed accounted for as much as 50% of all DNA–Cr adducts.

3. Chromium(V)

The complex $[CrCl(\mu\text{-}N^tBu)(2,6\text{-}^iPr_2C_6H_3N)]_2$ was synthesized from $CrCl_2(N^tBu)_2$ and the corresponding isocyanate [1]. The compound is diamagnetic as a result of spin-coupling via Cr–Cr bonding or the imido bridge. The dimer exhibits symmetric bridging with the Cr–N distances of 1.80 Å. The Cr–N(terminal amido) distance is 1.64 Å and Cr–Cl distances are 2.18 and 2.19 Å. The Cr···Cr distance is 2.49 Å and the Cr–N–Cr angles are 94 and 92°. Reaction of $CrCl_2(2,4,6\text{-}Me_3C_6H_2N)_2$ with MgEtBr in the presence of PMe_3 gives $(2,4,6\text{-}Me_3C_6H_2N)BrCr(\mu\text{-}2,4,6\text{-}Me_3C_6H_2N)_2CrBr(2,4,6\text{-}Me_3C_6H_2N)(PMe_3)$ [1]. The short Cr···Cr length (2.53 Å) and the Cr–N–Cr angles (85.5 and 86.6°) suggest some metal–metal bonding character. The bridges are unsymmetrical with the 5-coordinate (distorted trigonal bipyramidal) Cr–N(bridge) lengths 1.96 and 1.89 Å and the 4-coordinate (distorted tetrahedral) Cr–N(bridge) lengths 1.76 and 1.79 Å. The Cr–N(terminal imido) lengths are about equal for the 5- and 4-coordinate chromium (1.65 and 1.66 Å, respectively), whereas the Cr–Br lengths are significantly different (2.45 and 2.37 Å, respectively). The Cr–P bond length is 2.41 Å.

The crystal structure of $Ba_5[CrN_4]N$ was reported [14]. The chromium exhibits almost perfect tetrahedral coordination of the nitrido ligands. Two Cr–N distances are 1.758 Å and two are 1.753 Å. The distorted octahedral coordination spheres for the nitrido ligand are completed with five neighbouring Ba^{2+} ions. The overall structure is thus composed of tetrameric octahedra connected by common $CrBa_2$ faces and CrBa edges. The N^{3-} counterions are surrounded by an octahedron of Ba^{2+} ions. The $S=\frac{1}{2}$ spin state was confirmed by variable-temperature magnetic susceptibility measurements.

The structure of the nitrido complex Cr(bpb)N, where bpb^{2-} is 1,2-bis(2-pyridinecarboxamido)benzene (3), was determined at 120 K [15]. Theoretical electron density studies were performed on the complex. The results were compared with deformation density maps. The complex clearly contains three distinct types of Cr–N bonding: Cr–N(py) dative bonds, Cr–N(amido) σ bonds, and a Cr–N(nitrido) triple bond, $\sigma^2\pi^4$. The Cr exhibits a square pyramidal coordination geometry with the nitrido ligand at the apex. The Cr–N bond lengths are 1.555,

1.966 and 2.082 Å for the nitrido, amido, and py nitrogens, respectively. An unpaired electron resides in the non-bonding Cr d-orbital.

(3)
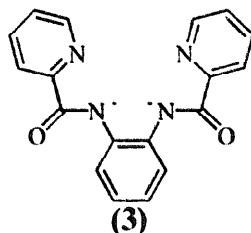
Calculations on $Cr(O_2)^+$ show that a bent structure, $\angle O{=}Cr{=}O = 109°$, has the minimum energy [16]. The cation was generated by the electron ionization of CrO_2Cl_2 and shown to oxidize ethene and propane through C–H and C–C bond activation. EPR Spectroscopy was used to examine the Cr(V) species generated by reaction of Cr(VI) with NADH/NADPH [17]. The Cr(V) species reacts with hydrogen peroxide to form hydroxyl radicals which subsequently attack the sugar and base moieties of DNA and RNA. The hydroxyl radical is generated as shown in either Eq. (2) or Eq. (3). Results suggest that the hydroxyl radical is the major agent involved in Cr-induced carcinogenesis.

$$Cr(V) + H_2O_2 \rightarrow Cr(V) \cdot H_2O_2 \rightarrow Cr(VI) + HO^\cdot + OH^- \qquad (2)$$

$$Cr(V) + H_2O_2 \rightarrow Cr(VI) + HO^\cdot + OH^- \qquad (3)$$
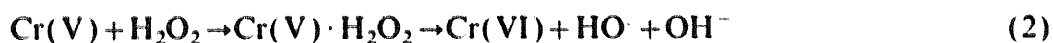
4. Chromium(IV)

The reaction of $CrCl_3(2,4,6\text{-}Me_3C_6H_2N)_2$ with $4\text{-}{}^tBuBzMgCl$ results in the formation of the imido bridged complex $\{CrCl(\mu\text{-}2,4,6\text{-}Me_3C_6H_2N)\text{-}[N(4\text{-}{}^tBuBz)(2,4,6\text{-}Me_3C_6H_2)]\}_2$ [1]. A crystal structure of the di-Et_2O solvate was determined. The molecule lies on a centre of symmetry and the symmetrical Cr–N(bridge) distances are 1.820 and 1.814 Å. The Cr–Cl distances are 2.211 Å. The Cr–N(amido) distances are 1.820 Å, which imply that a degree of multiple bonding exists. The Cr···Cr distance (2.512 Å) suggests some bonding interaction. The geometry about the Cr is essentially tetrahedral.

When heated in the presence of PMe_3, the arylimido Cr(IV) complexes $Cr(2,4,6\text{-}Me_3C_6H_2N)_2R_2$ ($R = CH_2CMe_3$, CH_2CMe_2Ph, or CH_2Ph) are reduced and the diamagnetic Cr(IV) dimer $[Cr(\mu\text{-}2,4,6\text{-}Me_3C_6H_2N)(2,4,6\text{-}Me_3C_6H_2N)\text{-}(PMe_3)]_2$ is isolated [1]. The complex was studied by ${}^1H$ and ${}^{31}P$ NMR spectroscopies. Two types of $2,4,6\text{-}Me_3C_6H_2N$ are clearly discernible in CD_2Cl_2. However, in d_8-thf there is evidence of free PMe_3 and decomposition products are observed with time. In the solid state, the dimer resides on a C_2 axis through and perpendicular to the Cr_2N_2 ring. The Cr coordination geometry is a highly distorted tetrahedron. The imido bridges are symmetrical with Cr–N(bridge) distances of 1.848 and 1.836 Å. The Cr–N(terminal imido) and Cr–P distances are 1.680 and 2.322 Å,

respectively. The short Cr⋯Cr distance (2.496 Å) and Cr–N–Cr angle (85.3°) suggest some Cr–Cr interaction.

The absorption spectra of Cr(IV) doped $ZrSiO_4$ have been studied [18]. Although in theory Cr^{4+} can replace either Zr^{4+} (dodecahedral site symmetry) or Si^{4+} (distorted tetrahedral site symmetry, D_{2d}), the authors deduce that the results are consistent with only Si^{4+} substitution by way of analogy with the spectra of Cr(IV) doped $Y_3Al_5O_{12}$.

5. Chromium(III)

5.1. Complexes with monodentate ligands

The anation reactions of complexes of the type $[Cr(NH_2R)_5(H_2O)]^{3+}$, R = H, Me or Pr, have been examined in an effort to gain insight into the effect of the size of R on the rate of reaction [19]. A definite decrease in the second-order rate constants is observed as the size of R increases. The data suggest that an increase in the steric demands of the spectator ligands results in an increase in the dissociative character of the mechanism.

The kinetics of Hg^{2+}-assisted chloride release from $[CrCl(NH_2R)_5]^{2+}$ complexes, where R = H, Me, Et, ^nPr, ^nBu, were studied [20]. In all cases examined, plots of $[Hg^{2+}]$ vs k_{obs} were linear and passed through the origin. As a result of the increase in activation enthalpy, a marked decrease was observed in the rate of Hg^{2+}-assisted reaction when R = H was compared to R = Me. This is in line with that observed for the thermal reaction. As the size of R progresses from Me to ^nBu, the values of $\Delta H^{\ddagger}$ and $\Delta S^{\ddagger}$ vary from 79 to 98 kJ mol^{-1} and -32 to $+21$ J K^{-1} mol^{-1}, respectively. Comparisons are made with the corresponding Co(III) salts. Changes in $\Delta H^{\ddagger}$ appear to be the dominant factor in influencing the decrease in the rate of reaction, as the relative $\Delta S^{\ddagger}$ changes are independent of the metal. The authors conclude that the R ≠ H systems all require about the same degree of structural reorganization in the initial stages of the interchange mechanism and so lie in about the same position in the interchange mechanistic continuum.

An efficient synthesis of salts of the complex ions trans-$[CrCl_2(NH_2R)_4]^+$, where R = Et, ^nPr or ^nBu, from $CrCl_3(thf)_3$ was reported [21]. The structure of trans-$[CrCl_2(NH_2^nPr)_4]BF_4 \cdot H_2O$ was determined. The complex cation exhibits Cr–Cl bond lengths of 2.326 and 2.324 Å and Cr–N bond lengths ranging from 2.110 to 2.113 Å. The thermal and Hg^{2+}-assisted chloride release kinetics for some of the complexes of the type trans-$[CrCl_2(N)_4]^+$ were also reported. The progress of the reaction was monitored spectrophotometrically. A change from R = H to R = Et results in a 16-times reduction in reaction rate. Differences in the absorption changes in comparing thermal to Hg^{2+}-assisted hydrolysis suggest that the thermal reaction may be complicated by a competitive amine loss. $\Delta S^{\ddagger}$ values range from +63 to -69 J K^{-1} mol^{-1} for the thermal acid hydrolysis process. The large range suggests significant variation in the extent of penetration of the water molecule occurring during the interchange process. Thus, although the non-replaced ligands do not have

a significant effect on the reactivity, they do influence the degree of $Cr-OH_2$ bond making in the transition state. However, in the case of Hg^{2+}-assisted chloride release, the non-replaced ligands have a considerable consequence on the rate. The rate is about 60-times faster when $R = H$ than when $R = {}^nPr$ or ${}^nBu$. Most of the determined $\Delta S^{\ddagger}$ values are in the range -30 ± 10 J K^{-1} mol^{-1}. The authors ascribe the difference in influence on $\Delta S^{\ddagger}$ associated with the non-replaced ligands to the better leaving-group character of $HgCl^+$ relative to Cl^-.

Polarographic and spectrophotometric studies of aqueous solutions of Hg^{2+} and $trans$-$Cr(NH_3)_4(CN)_2^+$ led to the identification of six Cr(III) species [22]. Evidence is presented for the formation of two trinuclear adducts with Cr:Hg proportions of 2:1 and 1:2. The formation of the adducts is accompanied by linkage isomerization of the cyanide bridging groups and Hg^{2+}-assisted aquation. Complete stereo-retention is maintained during the reactions. The palaeographic half-wave reduction potentials and UV–VIS spectra are reported for the $trans$ complex ions $[Cr(NH_3)_4(CN)_2]^+$, $[Cr(NH_3)_4(CN)(NC)]^+$, $[Cr(NH_3)_4(NC)_2]^+$, $[Cr(NH_3)_4(H_2O)(CN)]^{2+}$, $[Cr(NH_3)_4(H_2O)(NC)]^{2+}$, and $[Cr(NH_3)_4(H_2O)_2]^{3+}$. Qualitative rate data are reported for linkage isomerization and aquation.

The crystal structure of $[Cr(NH_3)_6][CuCl_5]$ was determined at 295 and 120 K [23]. At 295 K the salt exists in a cubic phase and at 120 K in a tetragonal phase. The geometry of the $[CuCl_5]^{3-}$ ion undergoes a change from D_{3h} to C_{2v} symmetry during the phase transition. The $[Cr(NH_3)_6]^{3+}$ ion exhibits a unique Cr–N distance of 2.074 Å in the cubic phase and unique Cr–N distances of 2.096, 2.066, and 2.083 Å in the tetragonal phase.

The selective broadening of certain ^{1}H NMR spectroscopic resonances by the redox-inactive paramagnetic complexes $[Cr(NH_3)_6]^{3+}$, $[Cr(en)_3]^{3+}$, and $[Cr(CN)_6]^{3-}$ was used to demonstrate dual-site activity on the blue copper protein amicyanin from $T.$ $versutus$ [24]. Resonances in the aromatic region and from δ 3.5 to -1.0 were only slightly broadened in the presence of $[Cr(NH_3)_6]^{3+}$ or $[Cr(en)_3]^{3+}$, but they were markedly broadened in the presence of $[Cr(CN)_6]^{3-}$. Most affected are resonances associated with His-54, His-96, Phe-98, Lys-59 and Lys-60. Inhibition studies on the oxidation of amicyanin by $[Fe(CN)_6]^{3-}$ by $[Cr(CN)_6]^{3-}$ were also performed. A two-site mechanism for the inhibition was demonstrated and rate data are reported. The NMR spectroscopic studies show that association of $[Cr(CN)_6]^{3-}$ is more favourable at the Phe-92 site. The authors deduce an electron transfer path from Phe-92 via Cys-93 to copper. This site is preferentially blocked by $[Cr(CN)_6]^{3-}$. The second site identified for electron transfer with $[Fe(CN)_6]^{3-}$ involves His-96, which is surrounded by an exposed hydrophobic patch and so is less inhibited by $[Cr(CN)_6]^{3-}$.

The bonding of chromium(III) nitrides was described in terms of a trigonal prismatic coordination geometry for the Cr(III) and a bent bond formalism for the nitride ligands [25]. As a result of the strong metal-nitrogen π-bonding, the complexes can be treated as trigonal prismatic, although the CrN_3^{6-} geometry observed in the solid state structure of the calcium salt is trigonal planar. The model allows for the accurate prediction of one unpaired electron.

The synthesis of $[Cr(NH_3)_6][Ln(dipic)_3]$, where Ln is a lanthanide and dipicH$_2$ is

pyridine-2,6-dicarboxylic acid, was reported [26]. The photophysical properties of these complexes were examined. A marked quenching of the anion luminescence results via a pathway involving the spin-forbidden Cr(III) d–d transitions.

The crystal structures of the weberites $Na_2M^{II}Cr^{III}F_7$, where M is Co or Fe, were reported [27]. The structures are similar to other weberites in most respects. The CrF_6 coordination geometry is distorted octahedral. The average Cr–F distances are 1.902 and 1.905 Å for the Co and Fe compounds, respectively, and the average M–F–Cr angles are 138.2° for both. The Na ions are surrounded by eight fluorides with the coordination geometry distorted between a cube and a hexagonal bipyramid.

The thermal decomposition of urea hexafluorochromate monohydrate and melammonium pentafluorochromate monohydrate and the solid state reaction of melamine and CrF_3 were investigated [28]. The results show that the amount of Cr^{2+} in the final product increases with an increase in final temperature. Formation of CrF_2 was observed only when the final step of the decomposition of the fluorochromates proceeded at temperatures greater than 700°C. The final product from the solid state reaction of melamine and CrF_3 was Cr_2F_5.

5.2. Complexes with didentate ligands

5.2.1. Oxygen donor ligand systems

The kinetics of ligand substitution were reported for cis-$Cr(ox)_2(H_2O)_2^-$ with SCN^- and N_3^-, $Cr(acac)_2(H_2O)_2^+$ with SCN^- and $Cr(atda)(H_2O)_2$ with SCN^-, where atda^{3-} is (4) [29]. The process occurs in two steps for each system. The proposed I_d mechanism involves the loss of one end of the chelate ligand as the first step.
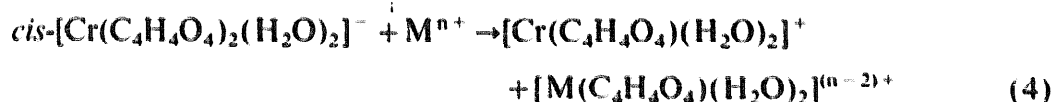

(4)
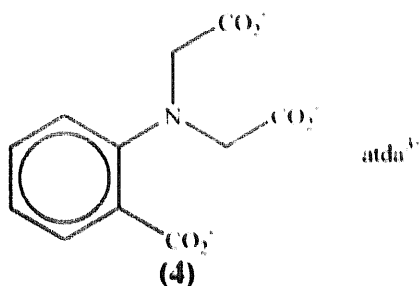
The ESR spectra of a number of hydroxamate complexes have been reported [30]. The complexes are of the form $Cr(RHA)_3$, where RHA is the hydroxamic acid derivative of acetic acid, cinnamic acid, mandelic acid and succinic acid. The magnetic susceptibilities are in the range of 3.01 to 3.87 μ_B. Data suggest that the complexes are more covalent than $Cr(H_2O)_6^{3+}$ but more ionic than $Cr(CN)_6^{3-}$. The covalent character follows the order R = malonato < aceto < succino < cinnamato. The complexes $Cr(A)^+$ and mixed ligand complexes of the type $Cr(A)(L)$, where H_2A is salicylic acid, 5-sulfosalicylic acid or 3,5-dinitrosalicylic acid and HL is a substituted glycine, have been studied using potentiometry [31]. The glycine analogues examined were the 3,5-dinitro, acetyl, phenylacetyl, 2-nitrobenzoyl, 4-nitrobenzoyl, 3-nitrobenzoyl, and benzoyl N-substituted derivatives. The stability

constants of the complexes and the proton dissociation constants of the ligands were reported.

The synthesis and thermogravimetric analysis of the tris(4-benzoyl-3-methyl-1-phenyl-2-pyrazolin-5-one) complex of Cr(III) were reported [32]. A strong endothermic peak corresponding to a phase change on melting was observed at 272°C. The complex undergoes an exothermic reaction at about 400°C, which was attributed to the decomposition of the ligand.

Spectral and electrochemical studies were performed on complexes formed between d-tartaric and dl-mandelic acids and Cr(III) [7]. The UV–VIS spectra obtained are consistent with octahedral coordination geometry. A pH dependence is observed, which was attributed to protonation of the ligands. CD spectra of the d-tartrate complexes show three pronounced Cotton effects in the range 390–416(+), 540–575(−) and 586–620(+) nm. A weak CD band was observed at 275–282(+) nm. The CVs of the tartrates and mandelates show three reductions. The tartrates are more easily reduced than the mandelates. The Cu(II), Al(III) and VO^{2+} catalysed aquation of cis-bis(methylmalonato)diaquochromate(III) was studied [33]. The stoichiometry of the aquation is described by Eq. (4).

$$cis\text{-}[Cr(C_4H_4O_4)_2(H_2O)_2]^- + M^{n+} \rightarrow [Cr(C_4H_4O_4)(H_2O)_2]^+$$
$$+ [M(C_4H_4O_4)(H_2O)_2]^{(n-2)+} \qquad (4)$$

The proposed mechanism involves a rapid protonation preequillibrium followed by a rate-determinining attack of water on the protonated intermediate. First order behavior was observed with $k_{obs} = k_0 + k_1[H^+] + k_2[M^{n+}]$; k_2 follows the order $Fe^{3+} \gg VO^{2+} > Al^{3+}$.

5.2.2. Nitrogen donor ligand systems

The effect of ligand distortion on doublet luminescence and absorption spectra was examined for a series of Cr(III) complexes [34]. The trans and cis isomers of $[Cr(tn)_2(NH_3)_2](ClO_4)_3$, where tn is 1,3-diaminopropane, were among those examined. The trans complex exhibits a solid state splitting (5 cm^{-1}) in addition to the expected doublet splitting (44 cm^{-1}) as a result of the presence of two crystallographically nonequivalent complex sites in the crystal.

The direct syntheses of the complexes $[CrCl_2(bpy)_2]ClO_4 \cdot 2H_2O$ and $[Cr(bpy)_3](ClO_4)_3 \cdot H_2O$ from $CrCl_3 \cdot 6H_2O$ and $[Ag(bpy)_2]ClO_4 \cdot 2H_2O$ were reported [35]. The silver complex serves as the source of the bidentate ligand and as a source of Ag^+ to aid in the chloride abstraction from the substitution inert Cr(III) chloride. The methodology was employed to synthesize a number of Cr(II) and Cr(I) complexes (see below).

The syntheses of a series of salts of $Ln(dipic)_3^{3-}$, where Ln(III) is a lanthanide metal and dipicH$_2$ is pyridine-2,6-dicarboxylic acid, have been reported [26]. The $Cr(NN)_3^{3+}$ salts, where NN is en or urea, were prepared. The photophysical properties of the complexes were examined. A marked quenching of the Ln ion luminescence results via a pathway involving the spin-forbidden Cr(III) d–d transitions. In $[Cr(urea)_3][Tb(dipic)_3]$, Cr(III) transfers excitation energy to the anion's excited

states from its higher levels while deactivating the Ln ion through its lower (doublet) states.

An examination of the photoaquation of cis-Cr(phen)$_2$Cl$_2^+$ was performed [36]. The authors suggest that the complex undergoes aquation by an associative mechanism to form cis-Cr(phen)$_2$Cl(H$_2$O)$^{2+}$ and cis-Cr(phen)$_2$Cl(OH)$^+$, which goes on to form Cr(phen)$_2$(H$_2$O)$_2^+$. The quantum yield is enhance by four-fold in the absence of oxygen. However, the study was complicated by the observation that the complex was observed to undergo a dark aquation under biological conditions. The rate of photoaquation is enhanced in the presence of deoxyguanosine, dG. Photolysis studies done in the presence of DNA show the formation of covalently bonded adducts, but the interaction is weak as judged by the inability to observe the chromium complex-dG adduct by HPLC. There is a clear preference observed for binding to purines when polyribonucleotides are compared.

5.2.3. Sulfur donor ligand systems

The synthesis and characterization of (ΛΔ){Cr[(+)(S)(S)Mebdtp]$_3$} and Λ(-)$_{589}$- and Δ(+)$_{589}${Cr[(+)(S)(S)Mebdtp]$_3$}, where Mebdtp- is (5a), were reported [37]. Results of CD studies of the formation and configuration inversion reactions were presented. Based on the CD spectra, the Λ-(S,S)(S,S)(S,S) absolute configuration was assigned to (−)$_{589}${Cr[(+)(S)(S)Mebdtp]$_3$}. Thermodynamically, the Λ isomer is favoured over the Δ isomer, suggesting that the chiral centre located at the end of the aliphatic chain exerts some chiral discrimination at the metal centre. All attempts to obtain crystals of Cr[(+)(S)(S)Mebdtp]$_3$ yielded a 1:1 mixture of the Λ-(S,S)(S,S)(S,S) and Δ-(S,S)(S,S)(S,S) diastereoisomers. The crystal structure of racemic Cr(ddtp)$_3$, where ddtp⁻ is (5b), was determined. The complex exhibits an average Cr–S bond length of 2.425 Å, O–P–O angle of 96.1°, S–P–S angle of 106.2° and bite dimension (S···S) of 3.21 Å. The chelate rings have dihedral angles of 83.4 and 97.1°. This structure was used to model the structure of Cr[(+)(S)(S)Mebdtp]$_3$.

Mebdtp⁻
(5a)

ddtp⁻
(5b)
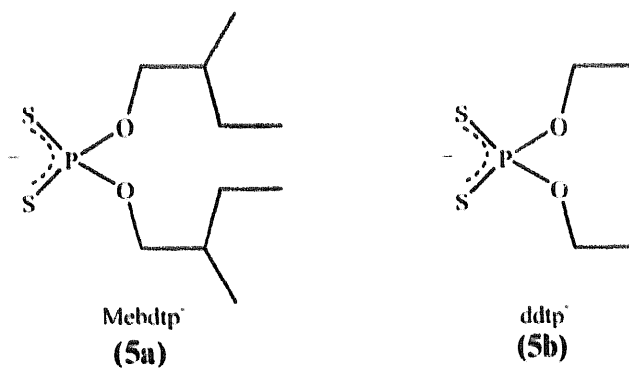
The crystal structure of the complex tris(O,O'-dicyclohexyldithiophosphato-S,S')chromium(III), Cr[S$_2$P(OC$_6$H$_{11}$)$_2$]$_3$, was reported [38]. The CrS$_6$ coordination sphere is a distorted octahedron with Cr–S distances ranging from 2.423 to 2.439 Å and S–Cr–S angles ranging from 81.4 to 81.7°.

5.2.4. Mixed donor ligand systems

The reaction of cis-[Cr(en)$_2$Cl$_2$]$^+$ with K$_2$SC$_2$O$_3$ was used to synthesize cis-[Cr(en)$_2$(SC$_2$O$_3$)]Cl [39]. The O,S chelation mode was confirmed by IR spectroscopy. The aquation of the complex was monitored by UV–VIS spectroscopy. The suggested mechanism involves the breaking of the Cr–S bond as the rate determining step. The final products of the aquation are en, H$_2$S, and cis-[Cr(H$_2$O)$_4$(C$_2$O$_4$)]$^+$.

The isomers Δ- and Λ-fac-[Cr(S-trp)$_3$], where S-trp is deprotonated (S)-tryptophan, were synthesized from [Cr(en)$_3$]$^{3+}$ and (S)-tryptophan [40]. The ligand S-trp coordinates via the lone pairs on the amine nitrogen and the carboxylic oxygen atoms. The stereoisomers were resolved via extraction with acetone. The assignment of the isomers as fac was based on a comparison of UV–VIS spectra with those of related Cr(AA)$_3$ systems. Based on the CD spectra, the acetone-soluble and -insoluble isomers were assigned the Δ and Λ absolute configurations, respectively. Δ-fac-[Cr(S-trp)$_3$] is photoinert upon d–d excitation, but the Λ isomer undergoes photoconversion to the Δ isomer with a quantum yield of 0.03. No fac→mer isomerization was observed, suggesting a Bailar twist mechanism for the photoinversion. Molecular mechanics calculations shown the Δ isomer to be more stable than the Λ isomer by about 7 kcal mol^{-1}.

The synthesis and characterization of the complex Cr(HBAB)$_3$ have been reported where H$_2$BAB is 5-(2-hydroxybenzylidene)aminobenzopyrazole, (6) [41]. From a comparison of the IR spectra of the ligand and the complex, the authors conclude that coordination takes place through the phenolic oxygen and the acyclic nitrogen. The complex exhibits a magnetic moment of 3.68 μ_B which, along with the UV–VIS absorption spectrum, are consistent with an octahedral ligand field.

(6)
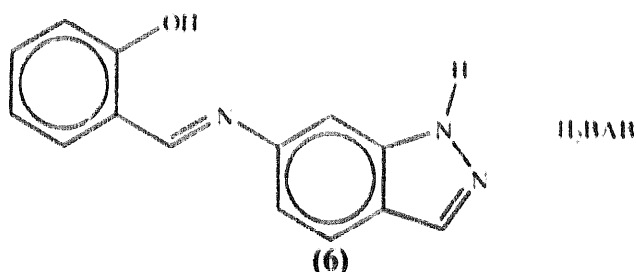
The reaction of CrCl$_3$py$_3$ or anhydrous CrCl$_3$ with nicotinic acid, glycine, L-cystine, L-cysteine, L-threonine or D-penicillamine in a 1:3 molar ratio results in the formation of a series of Cr(III) complexes [42]. The complexes exhibit magnetic moments in the range 3.4–4.05 μ_B. The UV–VIS spectra are consistent with pseudo-octahedral coordination geometries. The IR spectra are consistent with coordination via the amino and carboxylate groups. CD spectra suggest fac coordination for the threonine, cystine, and cysteine complexes but mer coordination for the penicillamine complexes.

The anation of [Cr(H$_2$O)$_6$]$^{3+}$ by lysine was investigated [43]. The reaction proceeds via an outer-sphere association of the ligand with Cr^{3+}/CrOH^{2+} followed by the transformation into an inner-sphere complex. The outer-sphere complex is stabilized by hydrogen bonding to a greater degree for the aqua complex as compared

to the hydroxy complex. The authors conclude that $[Cr(H_2O)_6]^{3+}$ reacts via an I_a path, but $[Cr(H_2O)_5(OH)]^{2+}$ reacts by an I_d path.

The magnetic properties of a number of Cr(III) complexes of amino acids were reported [44]. The amino acid complexes with the formulas $Cr(val)_3 \cdot 2H_2O \cdot KCl$, $Cr_2(tryp)_4Cl \cdot 2H_2O$, $Cr_2(glu)_3(OH)_2 \cdot 2H_2O \cdot KCl$, $K[Cr(cys)_2]$ $\cdot 4H_2O$, $Cr(ser)_3Cl_3 \cdot 3H_2O$, $Cr(his)_3Cl_3 \cdot 3H_2O$, and $Cr_2(met)_4Cl_2 \cdot 2H_2O \cdot KCl$ were investigated. For comparison with a compound having only carboxylate ligands, $Cr(ant)_3 \cdot H_2O$, where antH is anthranilic acid, was examined. The effective magnetic moment and the magnetic susceptibility are much smaller for $Cr_2(met)_4Cl_2 \cdot 2H_2O \cdot KCl$ than for the other complexes. EPR spectroscopic data for each compound are also reported. The data are consistent with a distorted octahedral field for each of the complexes.

Stability constants for coordination of 1,4-pyrazine-2-carboxylic acid, pcaH, and 3-amino-1,4-pyrazine-2-carboxylic acid, apcaH, to Cr(III) were determined [45]. The affinity of apca$^-$ is less than pca$^-$. This is attributed to hydrogen bonding between the carboxylate and amino groups. The log K_1 and log K_2 values obtained are 4.94 and 4.32 for pca and 4.14 and 3.20 for apca.

5.3. Complexes with polydentate ligands
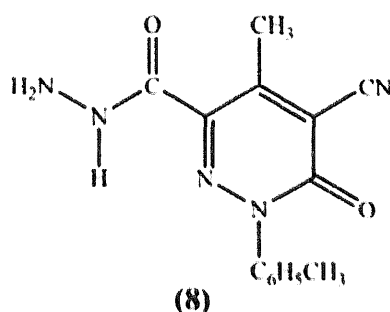
5.3.1. Tridentate ligands

The crystal structure of $[Cr(dpt)(glygly)]ClO_4 \cdot H_2O$, where dpt is bis(3-aminopropyl)amine and glyglyH$_2$ is glycylglycine (7), was determined [46]. The complex cation adopts the *mer* geometry. The Cr–N(glygly amine) and Cr–N(glygly amide) bond lengths are 2.11 and 1.96 Å, respectively, and the Cr–O bond length is 1.92 Å. The glygly N–Cr–N and N–Cr–O angles are 80.4 and 82.1°. The dpt N–Cr–N angles are 89.9 and 87.3°. The water bridges the perchlorate anion and the complex cation with hydrogen-bonding interactions involving the glygly peptide oxygen.

glyglyH$_2$

(7)
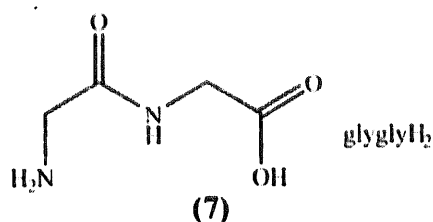
The effect of pressure on the rate of Hg^{2+}-assisted chloride release was examined for several *mer*-[CrCl(diamine)(triamine)]$^{2+}$ complexes [47]. The complexes were the $[ZnCl_4]^{2-}$ salts and the diamines examined were en, tn $= NH_2(CH_2)_3NH_2$, bn $= NH_2(CH_2)_4NH_2$, ibn $= NH_2C(CH_3)_2CH_2NH_2$, Me$_2$tn $=$ NH$_2$CH$_2$C(CH$_3$)$_2$CH$_2$NH$_2$ and NMetn $= CH_3NH(CH_2)_3NH_2$. The triamines examined were dien, 2,3-tri $= NH_2(CH_2)_2NH(CH_2)_3NH_2$, dpt $= NH_2(CH_2)_3NH(CH_2)_3$-NH$_2$, ampy and Medpt $= NH_2(CH_2)_3N(CH_3)(CH_2)_3NH_2$. The reactions were followed spectrophotometrically. The rate of Hg^{2+}-assisted chloride release varied by

10^4 and the correlation with thermal aquation is not consistent. Activation volumes are independent of temperature and $\Delta V^{\ddagger}$ are in the range $\pm 5\,\mathrm{cm}^3\,\mathrm{mol}^{-1}$. The authors conclude that the mechanism involves an interchange pathway and that the loss of chloride from the complexes (with and without Hg^{2+} assistance) proceeds via a spectrum ranging from dissociative activation through associative activation.

The complex $CrL_2Cl \cdot 4H_2O$, where HL is 5-cyano-1,6-dihydro-4-methyl-1-*p*-tolyl-6-oxopyridazine-3-carboxylic acid hydrazide (**8**), was characterized [48]. The authors conclude from potentiometric titrations and IR spectroscopy that the ligand coordinates via the NH_2, acyclic carbonyl and deprotonated CH_3 groups to form two stable chelate rings, one 5-membered and the other 6-membered. TG analysis confirms the presence of the waters of hydration and conductance studies show that the complex is a 1:1 electrolyte. The UV–VIS spectrum and the magnetic moment (3.4 μ_B) are consistent with a pseudo-octahedral coordination geometry.

(8)

5.3.2. Tetra-, quinque- and sexi-dentate ligands

A family of complexes with the formula $Cr(S_2N_2O_2)$, where $S_2N_2O_2$ is one of the thioethers represented by (**9**), was reported [49]. From magnetic moment measurements, the complexes have an $S = \frac{3}{2}$ ground state. The EPR spectra exhibit signals at $g = 5.6$–3.5 and $g \sim 2$ with strong rhombic distortion. All the complexes show a one-electron $Cr(III/II)$ wave with $E_{1/2}$ about -0.1 V vs SCE. The structure of the CH_2Cl_2 solvate of the complex with $R = Me$ and $x = 3$ was determined by X-ray crystallography. The asymmetric unit is composed of two molecules which differ in their configurations. The two thioethers sites in a given molecule have the same configuration, different from that in the other. The two chromium sites are also enantiomeric. However, the bond distances and angles in the two molecules are very similar. The coordination geometry is extremely distorted octahedral with the two sets of ligand O,N,S-donor atoms coordinating *mer*. The five-membered chelate rings comprised of N,O and N,S are nearly planar. The Cr–S distances are of two types in each molecule with averages of 2.418 and 2.447 Å. The average Cr–O and Cr–N distances are 1.95 and 1.98 Å, respectively.

Reversed-phase ion-pair chromatography has been used for the simultaneous separation and determination of $Cr(III)$, $Cr(VI)$ and common ions [8]. The Cr species form complexes with 1,2-diaminecyclohexane-*N,N,N',N'*-tetraacetic acid, DCTA. The detection limit was $8\,\mathrm{ng}\,\mathrm{mL}^{-1}$ for $Cr(III)$, respectively. Off-line

$S_2O_2N_2$
R = Me, Ph; x = 2, 3
(9)
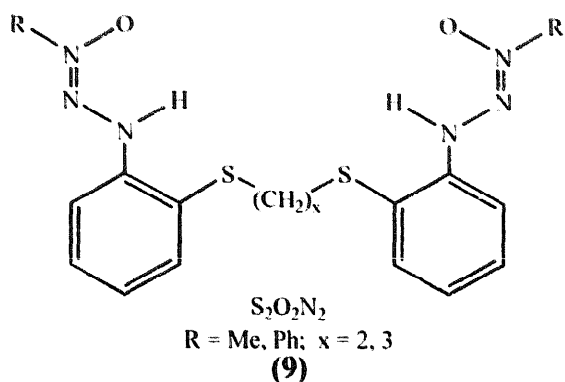
derivatization of Cr(III) was required because of the slow reaction times of the Cr with DCTA.

The synthesis of [Cr(sen)][Ln(dipic)$_3$], where Ln is a lanthanide, dipicH$_2$ is pyridine-2,6-dicarboxylic acid and sen is 1,1,1-tris(((2-aminoethyl)-amino)methyl)ethane, was reported [26]. The photophysical properties of these and similar complexes were examined. A marked quenching of the anion luminescence results via a pathway involving the spin-forbidden Cr(III) d–d transitions.

5.4. Complexes with macrocyclic ligands

To explore the possibility of stabilizing Cr(IV) and Cr(V) species, the complexes [Cr(L)(H$_2$O)$_2$]$^{3+}$, where L is the macrocycle (10), (11), (12), or cyclam, were examined by cyclic voltammetry [50]. The CV when L = (12) shows a single electron step corresponding to the formation of a Cr(IV) intermediate, suggesting that the Franck-Condon barrier is not as large as is the case for Cr(III/II) couples. The mechanism of oxidation with various oxidants was explored for various Cr(III) N$_4$-macrocyclic complexes. For oxidation of trans-[Cr(Schiff base)(H$_2$O)$_2$]$^+$, where Schiff base is salen or salpn, by Ce(IV), two-stage kinetics were observed. The first stage corresponds to the formation of a Cr(IV) intermediate and the second to the formation of a Cr(V) product. The authors postulate the formation of Cr(III)-L-Ce(IV) complex followed by intramolecular electron-transfer to form the Cr(IV) complex.

The syntheses of a series of salts of [Ln(dipic)$_3$]$^{3-}$, where Ln(III) is a lanthanide metal and dipicH$_2$ is pyridine-2,6-dicarboxylic acid, were reported [26]. The [Cr(sar)]$^{3+}$ salts, where sar is 3,6,10,13,19-hexaazabicyclo[6.6.6]icosane or the 1,8-diamino- or 1,8-dinitro- derivative of sar, were prepared. The photophysical properties of the complexes were examined. A marked quenching of the Ln(III) ion luminescence results via a pathway involving the spin-forbidden Cr(III) d – d transitions. The effect of ligand distortion on doublet luminescence and absorption spectra was examined for a series of Cr(III) complexes [34]. The macrocyclic complexes [Cr(L)]Br$_3$, where L = [18]aneN$_6$ = 1,4,7,10,13,16-hexaazacyclooctadecane, [20]aneN$_6$ = 1,4,7,11,14,17-hexaazacycloeicosane, sen = 4,4',4"-ethylidynetris(3-aza-butan-1-amine), and taptacn = 1,4,7-tris(aminopropyl)-1,4,7-triazacyclononane,

Me$_6$-[14]ane   Me$_6$-[14]diene   Me$_4$-[14]tetraene
(10)   **(11)**   **(12)**
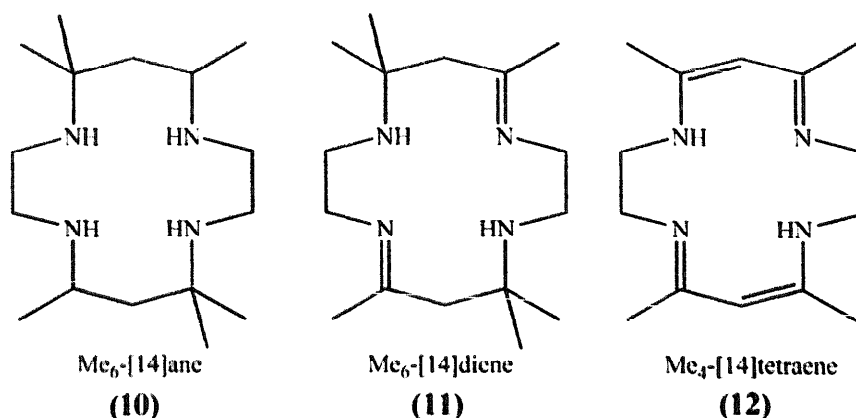
were examined. The ^2E_g electronic origins were assigned and found to split into two orbital components. The orbital splitting and the intensity distribution between the origin and vibronic sidebands was found to vary significantly, depending on the degree of deviation of the coordination environment from an exact inversion centre.

The crystal structures of Cr(tpp)(Cl)(L), where L = H$_2$O and py, were reported [51]. Cr(tpp)(Cl)(H$_2$O) resides on a C_4 axis passing through the O, Cr, and Cl atoms. The Cr–O and Cr–Cl bond distances are 2.239 and 2.242 Å. The Cr sits 0.035 Å above the N$_4$ core toward the water ligand. The unique Cr–N distance is 2.031 Å. The complex Cr(tpp)(Cl)(py) crystallizes with the py ligand rotated to give a dihedral angle of 3.7° with the plane defined by the *meso* carbon atoms and N(py). The Cr–Cl and Cr–N(py) distances are 2.311 and 2.140 Å. The Cr–N(porph) distances are 2.031, 2.021, 2.037, and 2.015 Å, with the Cr displaced by 0.063 Å from the N$_4$ core toward the Cl ligand. Laser flash photolysis studies of Cr(tpp)(Cl)(H$_2$O) and Cr(tpp)(Cl)(3-CNpy) were performed in toluene. The aqua complex exhibits transient spectra consistent with the loss of the water ligand. The photoreaction of the 3-CNpy complex proceeds with the formation of two distinct transients. The first transient (growth complete within 10^{-6} s) has a spectrum consistent with the formation of Cr(tpp)(Cl). The second transient ($t_{1/2} = 10^{-5}$ s) is attributed to Cr(tpp)(Cl)(H$_2$O). The quantum yields for photodissociation of the axial ligand at $\lambda_{exc} = 532$ nm for H$_2$O and 3-CNpy are 0.94 and 0.72, respectively.

The synthesis and crystal structure of *cis*-[CrCl$_2$([14]aneS$_4$)]PF$_6$, where [14]aneS$_4$ is (**13**), was reported [52]. The Cr atoms sits on a C_2 axis. The coordination geometry is distorted O_h with *cis* chloro ligands. The crystallographically unique Cr–Cl distance is 2.295 Å and Cr–S distances are 2.393 and 2.407 Å; the macrocycle adopts a folded conformation. The UV–VIS and IR spectra are consistent with a *cis* arrangement of chloro ligands in solution. The complex exhibits an irreversible wave assigned to Cr(III/II) at −0.75 vs Fe$^+$/Fe.

A series of complexes of Cr(III) with the formula CrLCl$_3$, where L is a potentially tetra-, penta- or hexadentate thioether ligand, have been characterized [53]. The electronic spectra were analysed and show that all of the thioethers function as weak field ligands toward Cr(III). The crystal structure of Cr(18S6)Cl$_3$, where 18S6 is (**14**), was determined. The complex exhibits trigonally distorted octahedral

[14]aneS$_4$

(13)
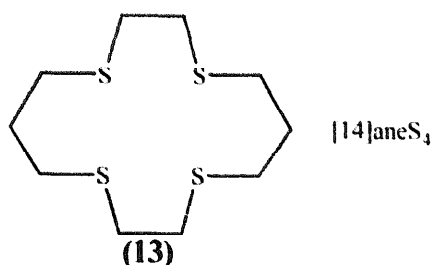
coordination with a *fac* arrangement of the three Cl ligands. Surprisingly, the thioether macrocycle coordinates in a tridentate fashion; the average Cr–Cl and Cr–S bonds are 2.292 and 2.447 Å, respectively. The similarity of the UV–VIS spectra show that a CrS$_3$Cl$_3$-coordination sphere is present for all of the complexes examined. As opposed to the situation with divalent metal ions or softer trivalent metal ions, the crown ethers which possess a large number of ethylene bridges provide the weakest ligand field.


18S6

(14)
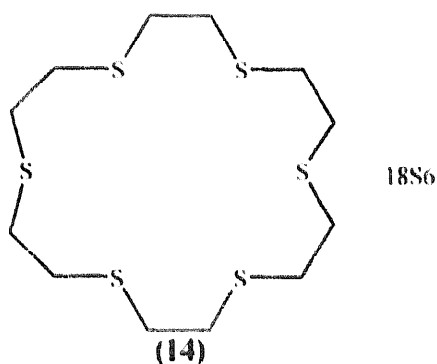
5.5. Dinuclear complexes

The synthesis and crystal structure of the formamidinate bridged complex (DTolF)$_2$Cr(μ-DTolF)$_2$(μ-Cl)$_2$Cr(DTolF), where HDTolF is *N,N'*-di-*p*-tolylformamidine, were reported [54]. A schematic representation of the molecule is shown in **(15)**. The complex was synthesized from the reaction of Cr$_2$(DTolF)$_4$ with PhICl$_2$. Single crystals of the complex obtained for X-ray analysis contain three molecules of benzene. The structure is best described as edge-sharing bioctahedral; the Cr···Cr distance is 2.889 Å. The complex sits on a centre of symmetry. The Cr–Cl distances are 2.345 and 2.355 Å, and the Cl–Cr–Cl and Cr–Cl–Cr angles are 104.13 and 75.87°, respectively. The Cr–N(bridge) distances are 2.071 and 2.057 Å and the Cr–N(terminal) distances are 2.051 and 2.030 Å. The N–Cr–N angle is 165.6° between the bridging formamidinates and the bite angle for the non-bridging chelate is 65.2°.

A novel metallamacrobicycle with the formula [LCr(μ-dmgH)(μ-dmg)CrL]$^+$, where L is 1,4,7-trimethyl-1,4,7-triazacyclononane, was reported [55]; a schematic representation of the structure is shown in **(16)**. The pK values corresponding to

R = p-tolyl

(15)
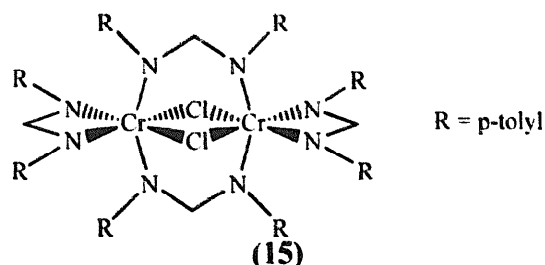
the deprotonation of dmgH ligands were found to be 10.72 and 4.39. The crystal structure of the MeOH solvate of the perchlorate salt was determined. The coordination geometry of the Cr(III) is a distorted octahedron with the three nitrogen atomss of the tridentate macrocycle on one face and a set of oxygen atoms from the two bridging $[dmg]^{2-}$ and $[dmgH]^{-}$ ligand forming the other face. The average Cr–N and Cr–O distances are 2.125 and 1.935 Å, and the Cr···Cr separation is 7.265 Å. The complex exhibits magnetic character consistent with antiferromagnetic coupling ($J = -4.7$ cm^{-1} and $g = 2.04$).

(16)
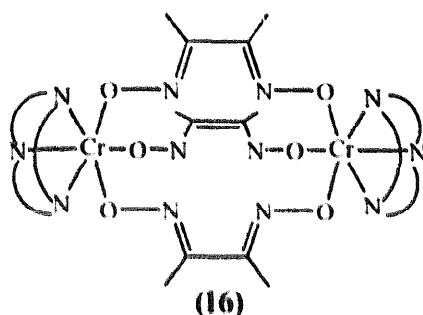
An investigation of a dinuclear Cr(III) complex bridged by diaminopyrine was performed [56]. A template synthesis employing Cr(III) salts, acetylacetone and 2,6-diaminopyridine was used to form the complexes $[Cr(acac_2dap)X]_2$ (17), where $X = Cl^-$, Br^-, NO_3^- and NCS^-. Based on elemental analysis, UV–VIS and IR spectral data, the coordination geometry was assigned as square pyramidal with coordination to the macrocycle as shown in (17). Variable temperature magnetic data yield magnetic moments in the range 4.20 to 3.86 μ_B.

The synthesis and kinetics of base hydrolysis of the hydroxide and carboxylate bridge complexes $[Cr_2(\mu\text{-OH})(\mu\text{-RCO}_2)(en)_4]^{4+}$ and $[(nta)Cr(\mu\text{-OH})(\mu\text{-RCO}_2)\text{-}Cr(en)_2]^+$, where nta is nitrilotriacetate and R = H, Me, ^nPr, CH_2Cl, CH_2ClCH_2, MeOCH or Ph, were reported [57]. Based on ^2H NMR spectroscopic data, only one isomer of $[(nta)Cr(\mu\text{-OH})(\mu\text{-RCO}_2)Cr(en)_2]^+$ is present and, by analogy with similar complexes for which X-ray structures are available, the authors argue that the bridging carboxylato ligand is cis to the tertiary amine nitrogen. The progress of reactions was monitored by UV–VIS and ^2H NMR spectroscopies. The hydrolysis occurs in two steps, only the first of which is dependent on R. For both complexes, reaction proceeds by a rapid initial deprotonation of the hydroxide to yield a μ-oxo species. Although $[Cr_2(\mu\text{-OH})(\mu\text{-RCO}_2)(en)_4]^{4+}$ undergoes cleavage at the carbox-

(17)
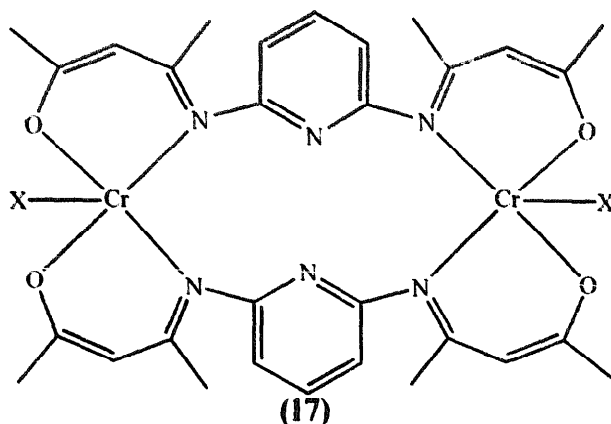
ylic acyl C–O bond, $[(nta)Cr(\mu\text{-OH})(\mu\text{-RCO}_2)Cr(en)_2]^+$ undergoes cleavage at the Cr–O bond on the $Cr(en)_2$ moiety.

A series of dinuclear chromium(III) complexes were prepared from the reaction of K_2CrO_4 and a group of saccharides and their derivatives [58]. The complexes were characterized by elemental analysis and various spectroscopic techniques. The complexes are anionic with the Cr(III) in a pseudo-octahedral geometry. Data suggest that both carboxylato and hydroxo ligation. Magnetic data show that the complexes exhibit antiferromagnetic character with $-2J$ varying from 10.0 to 25.0 cm^{-1}. CV experiments show that the Cr(III/II) reduction occurs in the range -1.1 to -1.4 V vs. Ag/AgCl. Some of the complexes exhibited one or two reversible Cr(III/IV) oxidation waves. Ab initio calculations were performed to examine the geometry dependence of magnetic exchange interactions in μ-oxo bridged Cr(III) complexes [59]. The complex $L_5Cr\text{-O-}CrL_5$ was used in the studies, where L is a He-like model ligand. The effects of Cr–O distance, Cr–O–Cr angle, and rotation of one CrL_5 group with respect to the other were examined. J drops off exponentially as the Cr–O distance increases. J is also quite dependent on the Cr–O–Cr angle and changes from strongly antiferromagnetic at 180° to ferromagnetic at angles near 120°. However, J is essentially independent of the rotation of the CrL_5 moiety.

5.6. Polynuclear complexes

The synthesis and structure of $(\mu_3\text{-oxo})$hexabenzoatotriamine trichromium(III) perchlorates were reported [60]. The complexes where the amine is pyridine, 2-, 3- or 4-picoline, 2,4-lutidine, quinoline, isoquinoline, morpholine or piperidine were synthesized by replacing the water ligands in the triaqua complex. The crystal structure of the piperidine complex was determined. The three Cr atoms lie on a mirror plane and are related by a 3-fold symmetry axis which passes through the μ_3-oxo ligand. The benzoate ligands bridge pairs of Cr atoms with three of the ligands on each side of the mirror plane. The Cr has a distorted tetragonal bipyramidal coordination sphere with a base composed two sets of symmetry related benzoic acid oxygen atoms and the apices composed of the oxo ligand and a piperidine ligand. The piperidine ligand is perpendicular to the mirror plane. The Cr–O(oxo)

distance is 1.913 Å and the Cr–N distance is 2.165 Å. The Cr–O(benzoate) bond distances are essentially the same: 1.970 and 1.969 Å. The OCrN angle is 174.2°. Two bands ($\sim 17\,000$ and $\sim 23\,000\,\text{cm}^{-1}$) and a shoulder ($\sim 15\,000$ to $15\,400\,\text{cm}^{-1}$) appear in the electronic absorption spectra of the complexes. Thermal gravimetric analyses suggest that amines substituted *ortho* to the nitrogen have weaker Cr–N bonds resulting from steric interactions. This is supported by shifts in the first band in the electronic absorption spectra.

The complexes $Cr_3O(O_2CR)_4(hq)_3$, where O_2CR is benzoate (O_2CPh) or acetate (O_2CCH_3) and 8-hydroxyquinoline (hqnH) or 5-chloro-8-hydroxy-quinoline (ClhqnH) were reported [61]. The crystal structure of $Cr_3O(O_2CPh)_4(hqn)_3 \cdot 1.25CH_2Cl_2$ was determined. The μ_3-oxo sits in the centre of a scalene triangle of Cr atoms. The Cr–O(μ_3-oxo) bond distances are 1.890, 1.963 and 1.978 Å; the Cr$\cdots$Cr distances are 2.909, 3.235 and 3.466 Å and the Cr–O–Cr angles are 94.4, 118.1, and 130.2°. The coordination of the Cr atoms is decidedly unsymmetrical with the two Cr atoms with the shortest internuclear separation spanned by a bridging benzoate ligand and a μ-O of an hqn ligand. The Cr atoms with the intermediate separation are bridged by two benzoate ligands and the Cr atoms with the longest separation are bridged by a single benzoate ligand. The remaining coordination sites are occupied by two didentate hqn ligands and the nitrogen of the hqn ligand that provides the bridging phenoxide atom. Magnetic susceptibility and EPR studies support antiferromagnetic exchange in the Cr_3O unit. Although at room temperature the coupling of the Cr atoms is weak (3.67 μ_B per Cr atoms), below 15 K the coupled total spin is consistent with $S = \frac{1}{2}$.

X-Ray absorption spectroscopic studies were used to examine polyhydroxy-(acetato)chromium(III) α-zirconium phosphates [62]. The precursors have connectivities of a flat dimer, a closed trimer, an open tetramer, and a fourth phase with connectivity between a trimer and tetramer. The flat dimer structure was deduced from XAFS data which revealed a CrO_6 shell having Cr–O distances of 1.97 Å and Cr atoms in the second coordination shell. The closed trimer structure is based on XAFS analysis which shows the first coordination shell of six oxygens at 1.97 Å and the second coordination shell of two Cr atoms at 3.06 Å. The authors conclude the most likely structure involves a $Cr_3(\mu_3\text{-OH})(\mu\text{-OH})_3$ unit. The open tetramer assignment is based on XAFS analysis that shows six oxygen atoms at 1.98 Å and three shells of Cr atoms at 2.95, 3.08 and ~ 3.6 Å with corresponding coordination numbers of 0.8, 1.5, and 1.5 Cr atoms. The suggested structure has two μ_3-OH and two μ_2-OH bridges, as shown in (18). XAFS data obtained for the fourth phase could be fit satisfactorily only by using parameters between those for an open tetramer and a trimer and the authors conclude that both tri- and tetra-nuclear clusters are present.

The anti-osteoporotic activity of a number of amine carboxyboranes, including $[Cr_3O\{(CH_3)_3BH_2COO\}_6(H_2O)_3]NO_3$, were examined [63]. The complexes were found to inhibit calcium flux from bone and macrophage cells, increase calcium uptake by the cells, and increase collagen synthesis in bone cells. Amine carboxybor-anes and their metal complexes were found to be inhibitors of enzymes involved in

(18)
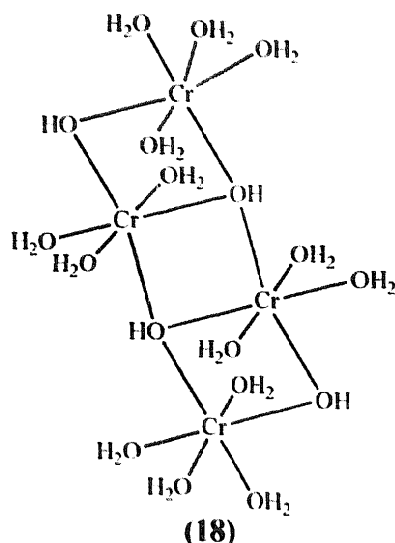
the synthesis of prostaglandins and leukotrienes, which are chemical mediators in the degradation of dense bone.

The synthesis of a series of trinuclear chromium(III) carboxylates via the reduction of $K_2Cr_2O_7$ with organic acids was reported [64]. The acids employed were phthalic (phtH$_2$), pyromellitic (pyrH$_4$) and glycine (glyH). Based on electronic and IR spectroscopies, thermogravimetric and X-ray powder diffraction analyses and magnetic susceptibility data, the structures were assigned. The complexes have the formulas $[Cr_3(\mu_3\text{-}O)(phtH)_4(pht)(OH)(H_2O)_3]\cdot 6H_2O$, $[Cr_3(\mu_3\text{-}O)(pyrH_2)\text{-}(pyrH_3)_5(H_2O)_3]\cdot 18H_2O$, and $[Cr_3(\mu_3\text{-}O)(gly)_6(H_2O)](CO_3)_{0.5}$. The carboxylate groups act as bridging ligands.

The structure of $[NEt_3H][Cr_4O_2(O_2CPh)_7(pic)_2]\cdot CH_2Cl_2$, where picH is picolinic acid, was determined [65]. The complex has a Cr_4O_2-unit in the core of the anion, which is composed of two edge-fused triangular Cr_3O units. The Cr_4 arrangement is of the butterfly type, and the hinge Cr atoms have an internuclear separation of 2.774 Å and are bridged by two μ-oxo ligands, which are also coordinated to the wingtip Cr atoms. The coordination is unsymmetrical with Cr–O(wingtip) = 1.864 Å and Cr–O(hinge) = 1.908 and 1.894 Å. Solution and solid-state magnetic susceptibility studies are consistent with antiferromagnetically coupled Cr centres. The magnetic moments at room temperature are 2.56 and 2.65 μ_B/Cr atom in the solid state and chloroform solution, respectively.

Two dioximato-bridged Cr(III)-Cu(II)-Cr(III) trinuclear complexes were reported [66]. The complexes have the formulas [Cr(salen)-Cu(BD)$_2$-Cr(salen)] (**19a**) and [Cr(salen)-Cu(FD)$_2$-Cr(salen)]·H$_2$O (**19b**) where BD^{2-} is α-benzyldioximato and FD^{2-} is α-furildioximato. Magnetic susceptibility data show that the Cr(III) and Cu(II) ions are ferromagnetically coupled via the oximato bridges.

EXAFS was used to study the structure of the metal-disordered complex $[Cr_2^{III}Co^{II}O(MeCO_2)_6(py)_3]\cdot py$ [67]. There is a 0.05 Å displacement of the μ_3-O away from the Co(II) towards the Cr(III)···Cr(III) midpoint. The Cr-μ_3-O and Co-μ_3-O distances are 1.95 and 1.87 Å and the Cr-μ_3-O-Cr and Co-μ_3-O-Cr angles

a   b

(19)
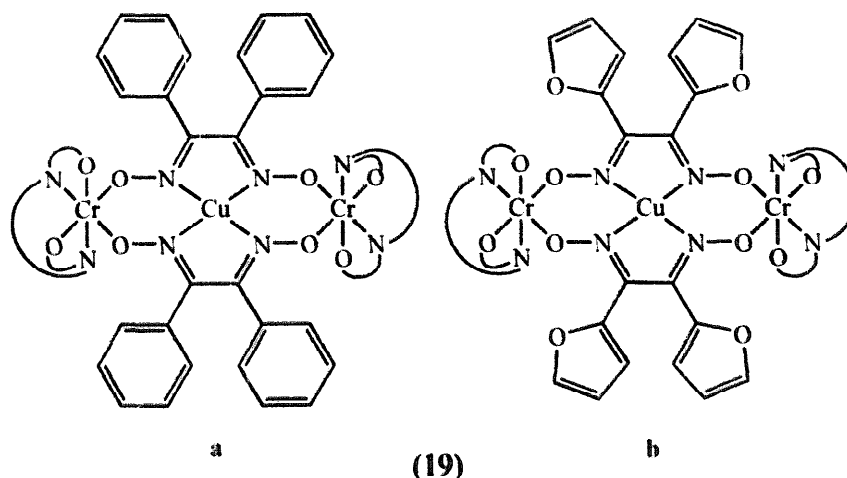
are 124 and 118°, respectively. The Cr_2CoO core is planar. The authors suggest that the observed increase in $Cr \cdots Cr$ antiferromagnetic coupling upon substitution of the third $Cr(III)$ with $Co(II)$ results from the displacement of the μ_3-O toward the $Cr \cdots Cr$ midpoint and the polarization of the in-plane p orbital of the oxygen because of the lower charge on $Co(II)$. This results in an increased p-dπ(in plane) overlap, destabilization of the corresponding antibonding molecular orbitals and decreased ligand field splitting.

Preliminary X-ray structural and magnetic data for the hexacyanometalate $[Cr(CN-Ni(tetren)_6](ClO_4)_9$, where tetren is tetraethylenepentaamine, were reported [68]. Disorder of the perchlorate anions limited the refinement of the structure, but the positions of heavy atoms and their nearest neighbours were determined. The model has six Cr–C–N–Ni linkages and the nickel atoms are coordinated to the five nitrogens of the tetren ligand. IR spectroscopic data are consistent with the proposed bridging mode of the cyanide ligands. Magnetic data are suggestive of short-range ferromagnetic interactions between $Cr(III)$ and $Ni(II)$ via the bridging cyanide ligands with $J = +16.8$ cm^{-1} and $g = 2.00$. Magnetization studies are consistent with an $S = \frac{15}{2}$ ground state. The syntheses and magnetic properties for the series of compounds $A^{II}[Cr^{III}(CN)_6]_2 \cdot 15\text{-}18H_2O$, where A = Ni, Co, Fe, Mn and Cr, and $CsA^{II}[Cr^{III}(CN)_6] \cdot 0\text{-}2H_2O$ were also reported.

The structure of a new form of $Cr(III)$ vanadate(V), $CrVO_4$-I, was determined from X-ray powder diffraction data [69]. The structure consists of an infinite network of Cr_4O_{16} clusters composed of four edge-sharing CrO_6 octahedra linked to the other cluster by VO_4 tetrahedra. (20) is a representation of the Cr_4O_{16} cluster. Each cluster is composed of two crystallographically independent Cr atoms, each with an irregular octahedron of O atoms. The average Cr–O distances are 1.98 and 1.97 Å. The compound exhibits antiferromagnetic ordering at temperatures less than 11 K.

The synthesis of the Keggin anion dimer $[\{A\text{-}\alpha\text{-}SiO_4W_9O_{30}(OH)_3\text{-}Cr_3\}_2(OH)_3]^{11-}$ from $[A\text{-}\alpha\text{-}SiO_4W_9O_{30}(OH)_3Cr_3(OH_2)_3]^{4-}$ was reported [70]. Condensation is believed to occur in three steps involving the sequential deprotonation of the bridging oxygens between corner-linked CrO_6 octahedra or edge-linked

(20)
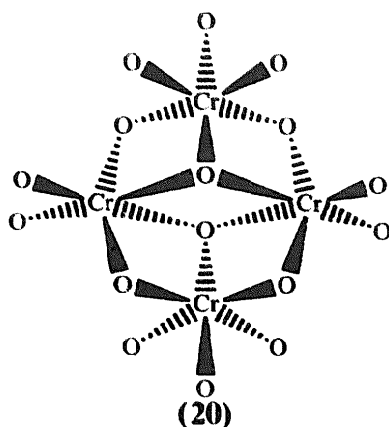
CrO_6-WO_6 octahedra, condensation of the resulting monomer units, and formation of hydroxo bridges between the monomeric units in the dimer. The crystal structure of the ammonium salt was obtained. The six Cr(III) ions form a trigonal prism with Cr–Cr distances of 3.62 Å in the monomer units and 3.61-3.62 Å between the dimer halves. The trigonal prismatic bridging unit is shown in (21). The Cr–OH–Cr angles are 135° in the dimer halves and 134 and 136° for the hydroxides bridging the two halves. The CrO_6 units are almost ideal octahedra. The structural features are compared to those of the monomer anion. Analysis of the temperature dependence of the ESR spectra gave a value of 60 ± 10 cm^{-1} for the antiferromagnetic coupling constant of the potassium salt of the dimer.

(21)
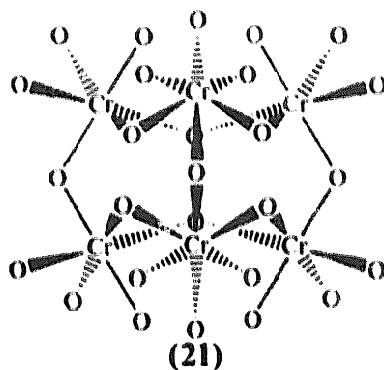
The formation of heteronuclear complexes of Cr(III) and Al was observed upon electrodeposition from a NaCl-KCl mixture containing $CrCl_3$ and $AlCl_3$ [71]. Voltammetry studies reveal two reversible reduction waves in the melt for Cr(III) in the absence of $AlCl_3$, which correspond to the sequential one electron process forming Cr(II) and two electron process to give Cr(0). Addition of $AlCl_3$ results in a reduction in peak heights and the appearance of a third wave between the first two. Upon addition of $AlCl_3$ to melts containing Cr(II) complexes, the formation of heterocomplexes is accompanied by the formation of elemental chromium. The quenched melt exhibits an ESR spectrum consistent with the increase in Cr(III) concentration with respect to Cr(II).

6. Chromium(II)

The crystal structures of the complexes all-*trans*-[CrCl$_2$(H$_2$O)$_2$(py)$_2$] and *trans*-[CrCl$_2$(py)$_4$]·acetone were reported [72]. As expected, each complex exhibits severe Jahn–Teller distortion along its Cl–Cr–Cl axis. For the diaqua complex, the Cr atom sits on a centre of symmetry and the unique Cr–Cl, Cr–O and Cr–N distances are 2.767, 2.066 and 2.127 Å, respectively. In the tetrapyridine complex, the unique Cr–Cl distance is 2.803 Å and the unique Cr–N distances are 2.160, 2.172 and 2.134 Å. In an effort to test the feasibility of predicting which set of bonds would be preferentially lengthened in Jahn–Teller distorted complexes, SCF-Xα-SW calculations were performed on the diaqua complex. Four structures were modelled using "normal" Cr–L distances, elongated Cr–Cl bonds, elongated Cr–O bonds and elongated Cr–N bonds. The results clearly predict that the lowest energy configuration has the Cr–Cl bonds lengthened when only the orbitals that are primarily d in character are considered. However, when the Cr–L bonding orbitals are taken into account, the calculated lowest energy configuration (by only 0.53 eV) is that with the elongated Cr–N bonds.

The bis(chlorosulfato) complex Cr(SO$_3$Cl)$_2$(pn)$_2$, where pn is 1,3-diaminopropane, and the tin adducts prepared by reaction with Me$_2$SnCl$_2$ or ^{n}Bu$_2$SnCl$_2$ in MeCN were reported [73]. The adducts are non-electrolytes and exhibit room temperature magnetic moments consistent with $S = 2$. Elemental analyses suggest a 1:2 stoichiometry, and IR spectra indicate covalently bonded, monodentate chlorosulfato groups.

The direct syntheses of the complexes CrCl$_3$(pap)$_2$ and CrCl$_3$(tap)$_2$, where pap and tap are 2-phenylazopyridine and 2-(*m*-tolylazo)pyridine, respectively, from CrCl$_3$·6H$_2$O and [Ag(pap)$_2$][ClO$_4$] or [Ag(tap)$_2$][ClO$_4$] were reported [35]. The silver complex serves as the source of the didentate ligand and as a source of Ag$^+$ to aid in the chloride abstraction from the substitution inert Cr(III) chloride. The strong π-accepting abilities of the pap and tap ligands stabilize the metal in the +2 oxidation state. The compounds exhibit a one-electron oxidation and a one-electron reduction. The room temperature magnetic susceptibilities are consistent with the low-spin state. The methodology was employed to synthesize a number of Cr(III) and Cr(I) complexes (see below).

The macrocyclic ligand 5,12-dioxa-7,14-dimethyl-1,4,8,11-tetraazacyclotetradeca-1,8-diene, (**22**), and its dichlorochromium(II) complex were isolated [74]. The complex is a non-electrolyte. The room temperature magnetic moment and electronic spectrum are consistent with pseudo-octahedral coordination geometry.

The Cr–O and O–O bonding in the complexes [(H$_2$O)$_5$CrO$_2$]$^{2+}$ and [(H$_2$O)(cyclam)CrO$_2$]$^{2+}$ were studied using UVRR spectroscopy [75]. The results support the assignment of the Cr–O$_2$ bonding as Cr(III)–O$_2^-$, i.e., η^1-superoxochromium(III). When vibrational data are compared, the cyclam ligand is seen to decrease the Cr–O and O–O bond energies. Upon excitation of the LMCT band, both complexes undergo bond homolysis to give Cr(II) and O$_2$.

The complexes Cr^{II}(TPP) and Cr^{II}(OEP) were shown to undergo oxygen atom transfer from [Mo^{V}O(TPP)]$_2$O to form the corresponding Cr^{IV}oxo porphyrin and

(22)
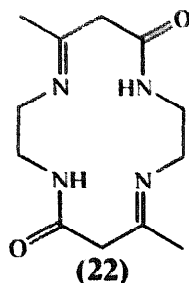
$Mo^{IV}O(TPP)$ [76]. When excess $Cr^{II}(TPP)$ was present, the μ-oxo Cr(III) porphyrin was produced. There was no evidence for the formation of bridged, mixed-metal complexes.

The reaction of Cr(II) with ethyliodoacetate and iodoacetatopentaammine-cobalt(III) were studied [77]. The reaction with ethyliodoacetate results in the formation of $[(H_2O)_5CrI]^{2+}$ and $[(H_2O)_5CrCH_2CO_2C_2H_5]^{2+}$. The formation of $[(H_2O)_5CrI]^{2+}$ is followed by its Cr^{2+} catalysed aquation. The aquation of the iodo complex was verified by independent aquation studies. The reaction with the cobalt(III) complex is biphasic. One route leads to the formation of Co^{2+} and the acetato coordinated Cr(III) species which reacts further to give $[(H_2O)_5CrI]^{2+}$ and $[(H_2O)_5Cr-OC(O)CH_2-Cr(H_2O)_5]^{4+}$. The other pathway gives $[(H_2O)_5CrI]^{2+}$ and $[(NH_3)_5Co-OC(O)CH_2-Cr(H_2O)_5]^{4+}$, which reacts further with Cr^{2+} to give $[(H_2O)_5Cr-OC(O)CH_2-Cr(H_2O)_5]^{4+}$ and Co^{2+}. Kinetic and activation parameters were reported.

7. Chromium(I)

The syntheses of $[Cr(pap)_3][ClO_4] \cdot H_2O$, $[Cr(tap)_3][ClO_4] \cdot H_2O$, $[Cr(pap)_2(bpy)]-[ClO_4] \cdot H_2O$ and $[Cr(pap)_2(bpy)][ClO_4] \cdot H_2O$, where pap and tap are 2-phenyl-azopyridine and 2-(m-tolylazo)pyridine, respectively, from $CrCl_3 \cdot 6H_2O$, $CrCl_2(pap)_2$ or $CrCl_2(tap)_2$ and $[Ag(pap)_2]ClO_4$ or $[Ag(tap)_2]ClO_4$ were reported [35]. The silver complex serves as the source of the didentate ligand and as a source of Ag^+ to aid in the chloride abstraction from the substitution inert Cr(III) chloride. The remarkable stability of these Cr(I) complexes is attributed to the strong π-accepting abilities of the pap and tap ligands. A voltammetric analysis showed that these compounds exhibit two one-electron oxidations and one one-electron reduction. The room temperature magnetic susceptibilities are consistent with a t_2^5 ground state. The same methodology was employed to synthesize a number of Cr(III) and Cr(II) complexes (see above).

8. Mixed valence complexes

The electrochemistry of chromium(II) hexacyanochromate(III) and iron(II) hexacyanochromate(III) immobilized on a graphite electrode was examined [78].

The Cr(II) system exhibits a reversible one-electron process corresponding to the reduction of the Cr coordinated to the carbon. The potential varies from -0.949 to -0.716 V vs. Ag/AgCl as the electrolyte is changed for the series $LiNO_3$, $NaNO_3$, KCl, RbCl and CsCl, supporting the suggestion that the reduction is accompanied by intercalation of cations. Only a very weak, irreversible peak at 1.00 V vs. Ag/AgCl is observed for the Cr coordinated to the nitrogen. For the Fe(II) system, isomerization to Cr(III) hexacyanoferrate(II) occurs upon reduction. The isomerization was followed by cyclic voltammetry. A redox wave observed at about -1.1 V vs. Ag/AgCl is gradually replaced by a wave at about 0.65 V vs. Ag/AgCl with an electrolyte consisting of 0.1 M KCl. The isomerization is believed to proceed by the initial formation of labile Cr(II), replacement of cyanide with water as the bridging ligand, and replacement of the bridging water with the Cr–NC–Fe linkage.

Electroreduction of acidic Cr(VI) solution at $+0.150$ V vs. SCE was shown to produce a brown, 1:1 Cr(III):Cr(VI) adduct [79]. XPS analysis revealed $2p_{3/2}$ binding energies of 579.0 and 581.3 eV, corresponding to Cr(III) and Cr(VI), respectively. The relative peak area for the Cr(III) was 1.05 with respect to Cr(IV). Upon leaching with hydroxide, a green deposit is formed. The alkali-leached deposit exhibits $2p_{3/2}$ binding energies of 579.0 and 580.8 eV, corresponding to Cr(III) and Cr(VI), respectively. The relative peak area for the Cr(III) was 2.18 with respect to Cr(IV). Treatment with alkali thus results in dissolving the Cr(VI) component to yield a 2:1 adduct.

The synthesis and magnetic characterization of the $N(^nBu)_4^+$ and PPh_4^+ salts of $Cr^{II}Cr^{III}(C_2O_4)_3$ were reported [80]. Based on X-ray powder diffraction studies, the compounds are isostructural with the corresponding $Mn^{II}Cr^{III}$ compounds. Both salts exhibit antiferromagnetic interactions. In neither compound is a transition to a long range ordered state observed above 2 K. However, deviation from Curie–Weiss behaviour is observed below 100 K. The magnetic properties are contrasted with $Cr_3^{II}[Cr^{III}(CN)_6]_2 \cdot 10H_2O$. The differences are rationalized based on structural differences: in the cyanide, the lattice connectivity is three-dimensional near cubic and in the oxalate it is two-dimensional hexagonal. The Jahn–Teller distortion is trigonal in the oxalates but tetragonal in the cyanide.

References

[1] A.A. Danopoulos, G. Wilkinson, T.K.N. Sweet, M.B. Hursthouse, J. Chem. Soc., Dalton Trans., (1995) 2111.
[2] M.P. Coles, C.I. Dalby, V.C. Gibson, W. Clegg, M.R.J. Elsegood, Polyhedron 14 (1995) 2455.
[3] W.-H. Leung, M.-C. Wu, T.-C. Lau, W.-T. Wong, Inorg. Chem. 34 (1995) 4271.
[4] F. Benetollo, G. Bombieri, P. Gilli, P.M. Harlo, A. Polo, L.M. Vallarino, Polyhedron 14 (1995) 2255.
[5] J.D. Ayala, G. Bonbieri, F. Benetollo, P. Gilli, L.M. Vallarino, J. Chem. Crystallogr. 25 (1995) 355.
[6] L.A. Groat, A.C. Roberts, Y. Le Page, Can. Mineral. 33 (1995) 41.
[7] M.S. El-Shahawi, S.A. Barakat, Spectrochimica Acta 51A (1995) 171.
[8] A. Padarauskas, G. Schewdt, Talanta 42 (1995) 693.
[9] S.P. Kaiwar, C.P. Rao, Chem. Biol. Interact. 95 (1995) 89.

[10] P.C. Fresco, F. Shacker, A. Kortenkamp, Chem. Res. Toxicol. 8 (1995) 884.

[11] C. Karunakaran, P. Muthukumar, B. Muthukumaran, Oxid. Commun. 18 (1995) 56.

[12] M. Capellmann, A. Mikalsen, M. Hindrum, J. Alexander, Carcinogenesis 16 (1995) 1135.

[13] A. Zhitkovich, V. Voitkun, M. Costa, Carcinogenesis 16 (1995) 907.

[14] A. Tennstedt, R. Kniep, M. Hüber, W. Haase, Z. Anorg. Allg. Chem. 621 (1995) 511.

[15] C.-C. Wang, Y. Wang, L.-L. Chou, C.-M. Che, J. Phys. Chem. 99 (1995) 13899.

[16] D. Schröder, A. Fiedler, W.A. Herrman, H. Schwarz, Angew. Chem. Int. Ed. Engl., 34 (1995) 2517. [Angew. Chem., 107 (1995) 2714.]

[17] M.J. Molyneux, M.J. Davies, Carcinogenesis 16 (1995) 875.

[18] A. Belleti, R. Borromei, L. Oleari, Inorg. Chim. Acta 235 (1995) 349.

[19] G. González, M. Martinez, Inorg. Chim. Acta 230 (1995) 67.

[20] J. Wang, D.A. House, Inorg. Chim. Acta 233 (1995) 25.

[21] D.A. House, J. Wang, M. Nieuwenhuyzen, Inorg. Chim. Acta 237 (1995) 37.

[22] M. Rievaj, D. Bustin, P. Riccieri, E. Zinato, Inorg. Chim. Acta 228 (1995) 153.

[23] S. Ohba, T. Fujita, I. Bernal, Acta Crystallogr., Sect. C C51 (1995) 1481.

[24] C. Dennison, P. Kyritsis, R.P. Kalverda, G.W. Canters, W. McFarlane, A.G. Sykes, J. Chem. Soc., Dalton Trans., (1995) 3395.

[25] R.B. King, Can. J. Chem. 73 (1995) 963.

[26] P.A. Brayshaw, J.-C.G. Bünzli, P. Froidevaux, J.M. Harrowfield, Y. Kim, A.N. Sobolev, Inorg. Chem. 34 (1995) 2068.

[27] B. Peschel, M. Molinier, D. Babel, Z. Anorg. Allg. Chem. 621 (1995) 1573.

[28] D.-H. Menz, B. Ehrhardt, U. Calov, J. Therm. Anal. 44 (1995) 179.

[29] D. Banerjea, B. Chakravarti, Inorg. Chim. Acta 240 (1995) 117.

[30] P.V. Khadikar, A.K. Joshi, Chim. Acta Turc. 23 (1995) 95.

[31] V. Kolhe, V. Dhingra, K. Dwivedi, Orient. J. Chem. 11 (1995) 99.

[32] Y. Akama, S. Yajima, J. Therm. Anal. 44 (1995) 1107.

[33] M. J. Oh, J.-H. Lee, H.-J. Park, S.-K. Choi, Bull. Korean Chem. Soc. 16 (1995) 555.

[34] A.D. Kirk, P. Hoggard, H.U. Güdel, Inorg. Chim. Acta 238 (1995) 45.

[35] W. Kharmawphlang, S. Choudhury, A.K. Deb, S. Goswami, Inorg. Chem. 34 (1995) 3826.

[36] M.A. Billadeau, H. Morrison, J. Inorg. Biochem. 57 (1995) 249.

[37] P. Biscarini, R. Franca, R. Kuroda, Inorg. Chem. 34 (1995) 4618.

[38] R.-G. Xiong, X.-Z. You, Acta Crystallogr., Sec. C C51 (1995) 2484.

[39] Z. Chong, Y.-J. Zhang, Y. Gung, Y. Wu, Polyhedron 14 (1995) 3611.

[40] N.A.P. Kane-Maguire, T.W. Hanks, D.G. Jurs, R.M. Tollison, A.L. Heatherington, L.M. Ritzenthaler, L.M. McNulty, H.M. Wilson, Inorg. Chem. 34 (1995) 1121.

[41] T.A. Khan, M.A. Khan, M.M. Haq, Indian J. Chem., Sec. A 34A (1995) 655.

[42] M.S. El-Shahawi, Spectrochimica Acta 51A (1995) 161.

[43] Kabir-ud-Din, G.J. Khan, Proc. Indian Acad. Sci, Chem. Sci., 107 (1995) 11.

[44] K. Gielzak, W. Wojciechowski, Chem. Papers 49 (1995) 54.

[45] N.M. El-Guindi, H.B. Hassib, Arabian J. Sci. Eng. 20 (1995) 549.

[46] J.-H. Choi, I.-H. Suh, S.-H. Kwak, Acta Crystallogr., Sec. C. C51 (1995) 1745.

[47] D.A. House, R. van Eldik, Inorg. Chim. Acta 230 (1995) 29.

[48] M.M. Shoukry, A.K. Abdel Hadi, W.M. Hosny, S.M. Shouheib, Indian J. Chem., Sect. A 34A (1995) 716.

[49] S. Pattanayak, D.K. Das, P. Chakraborty, A. Chakravorty, Inorg. Chem. 34 (1995) 6556.

[50] R. Ramasami, B.U. Nair, M. Kanthimathi, C.K. Ranganathan, Proc. Indian Acad. Sci. (Chem. Sci.) 107 (1995) 411.

[51] M. Inamo, M. Hoshino, K. Nakajima, S. Aizawa, S. Funahashi, Bull. Chem. Soc. Jpn. 68 (1995) 2293.

[52] N.R. Champness, S.R. Jacob, G. Reid, Inorg. Chem. 34 (1995) 396.

[53] G.J. Grant, K.E. Rogers, W.N. Setzer, D.G. VanDerveer, Inorg. Chim. Acta 234 (1995) 35.

[54] F.A. Cotton, D.J. Maloney, J. Su, Inorg. Chim. Acta 236 (1995) 21.

[55] D. Burdinski, F. Birkelbach, M. Gerdan, A.X. Trautwein, K. Wieghardt, P. Chaudhuri, J. Chem. Soc., Chem. Commun., (1995) 963.

[56] D.P. Singh, V.B. Rana, Polyhedron 14 (1995) 20.

[57] T. Fujihara, Y. Abe, S. Kaizaki, J. Chem. Soc., Dalton Trans., (1995) 1823.

[58] S. Kaiwar, M.S.S. Raghaven, C.P. Rao, J. Chem. Soc., Dalton Trans., (1995) 1569.

[59] C. Wang, K. Fink, V. Staemmler, Chem. Phys. 201 (1995) 87.

[60] M.D. Revenko, G.A. Timko, A.K. Ursu, M.D. Mazus, V.Kh. Dravtsov, V.K. Rotaru, Russ. J. Coord. Chem., 21 (1995) 444. [Koord. Khim., 21 (1995) 463.]

[61] M.K. Nagi, A. Harton, S. Donald, Y.-S. Lee, M. Sabat, C.J. O'Connor, J.B. Vincent, Inorg. Chem. 34 (1995) 3813.

[62] D.J. Jones, J. Roziére, P. Maireles-Torres, A. Jiménez-López, P. Olivera-Pastor, E. Rodriguez-Castellón, A.A.G. Tomlinson, Inorg. Chem. 34 (1995) 4611.

[63] K.G. Rajendran, A. Sood, B.F. Spielvogel, I.H. Hall, V.M. Norwood III, K.W. Morse, App. Organomet. Chem. 9 (1995) 111.

[64] D. Vasovic, D. Poleti, D. Jancic, J. Serb. Chem. Soc. 60 (1995) 105.

[65] S. Donald, K. Terrell, J.B. Vincent, K.D. Robinson, Polyhedron 14 (1995) 971.

[66] S.-W. Zhang, D.-Z. Liao, Z.-H. Jiang, G.-L. Wang, Transition Metal Chem. 20 (1995) 396.

[67] A.B. Edwards, J.M. Charnock, C.D. Garner, A.B. Blake, J. Chem. Soc., Dalton Trans., (1995) 2515.

[68] T. Mallah, S. Ferlay, C. Auberger, C. Hélary, F. L'Hermite, R. Ouahès, J. Vaissermann, M. Verdaguer, P. Veillet, Mol. Cryst. Liq. Cryst. 273 (1995) 141.

[69] M. Touboul, S. Denis, L. Seguin, Eur. J. Solid State Inorg. Chem. 32 (1995) 577.

[70] K. Wassermann, R. Palm, H.-J. Lunk, J. Fuchs, N. Steinfeldt, R. Stösser, Inorg. Chem. 34 (1995) 5029.

[71] S.A Kuznetsov, A.L. Glagolevskaya, Russ. J. Electrochem., 31 (1995) 1285. [Elektrokhimiya, 31 (1995) 1389.]

[72] F.A. Cotton, L.M. Daniels, X. Feng, D.J. Maloney, C.A. Murillo, L.A. Zúñiga, Inorg. Chim. Acta 235 (1995) 21.

[73] M. Shakir, S. Hameed, F. Firdaus, S.P. Varkey, Transition Metal Chem. 20 (1995) 142.

[74] M. Shakir, S.P. Varkey, T.A. Khan, Indian J. Chem. 34A (1995) 72.

[75] A. Bakac, S.L. Scott, J.H. Espenson, K.R. Rodgers, J. Am. Chem. Soc. 117 (1995) 6483.

[76] S. Yamashita, T. Imamura, Y. Sasaki, Chem. Lett., (1995) 417.

[77] A.D. Jordan, S.L. Scott, R.B. Jordan, Inorg. Chim. Acta 239 (1995) 99.

[78] A. Dostal, U. Schröder, F. Scholz, Inorg. Chem. 34 (1995) 1711.

[79] D.R. Rosseinsky, G.K. Muthakia, C.L. Honeybourne, R.J. Ewen, Transition Metal Chem. 20 (1995) 88.

[80] C.J. Nuttall, C. Bellito, P. Day, J. Chem. Soc., Chem. Commun., (1995) 1513.